Int. J. Aquat. Biol. (2026) 14(3): 121-135
ISSN: 2322-5270; P-ISSN: 2383-0956
Journal homepage: www.ij-aquaticbiology.com

Original Article

Salt stress-driven bioorganic biorefinery of *Monoraphidium contortum* algae: Lipid transformation and starch valorization for integrated biodiesel and bioplastic production

Muntaha Mahmoud Al-Rashidy[1], Mira Ausama Al-Katib[2], Mohanad Yakdhan Saleh[*3]

[1]Nineveh Education Directorate, Iraqi Ministry of Education, Nineveh, Iraq.
[2]Department of Biology, College of Education for Pure Science, University of Mosul, Mosul, Iraq.
[3]Department of Chemistry, College of Education for Pure Science, University of Mosul, Mosul, Iraq.

Abstract: This study aimed to collect and identify *Monoraphidium contortum* from local water bodies in Mosul, Iraq, using morphological and molecular characteristics. Furthermore, after cultivation in multiple media (modified NPK and modified CH10) and exposure to saline stress, lipid transformation and starch valorization were estimated to support the integrated production of biodiesel and bioplastics. Based on the results, the best medium for growth was M4 (CaCO3 + (NPK20:20:20) + CH10). On the twelfth day, the light absorption reached 650 nm with an optical density of 1.742 in this medium. The extracted oil yield was 9.6%, and polyunsaturated fatty acids increased to 22.7%, which were used to produce biodiesel. The transesterification process successfully converted the crude oil into diesel in two stages: an acidic and a basic stage. GC-MS analyses revealed that the salt stress stimulated the algae to accumulate polyunsaturated fatty acids. FTIR showed the success of the reaction through the appearance of a peak. The carbonyl group of methyl esters at 1728 cm^{-1} and the disappearance of the glycerol and water fractions indicate the product's purity. HPLC results revealed that glucose was the main starch component at 55.48%, with 32.18% fructose and 12.34% sucrose. Furthermore, bioplastics were manufactured from the extracted starch, with glycerin added as a plasticizer. The results showed the high biodegradability of the manufactured plastic in soil, reaching a decomposition rate of 68.2% within 120 days, ASTM D6400, making it a successful, environmentally friendly product that conforms to international standards.

Article history:
Received 23 April 2026
Accepted 10 June 2026
Available online 25 June 2026

Keywords:
Microalgae
Salt stress
Biodiesel
Bioplastics

Introduction

As traditional energy sources, such as fossil fuels, decline, the search has intensified for renewable, clean energy sources and for ways to obtain them at lower cost. These sources are also important for climate change mitigation by reducing environmental pollution and greenhouse gas emissions (Benouis et al., 2022; Malla et al., 2023; Aziz et al., 2024). Algae are among the most important sustainable resources. There are large, multicellular algae, such as marine algae, and small, unicellular algae, found across the globe (Lee, 2018; Rashid et al., 2024; Hassan et al., 2025). The growth and performance of photosynthetic organisms are strongly influenced by environmental conditions, such as salinity and pollution, which can affect germination, growth patterns, and morphology, illustrating how environmental stress can alter biological development and productivity. These observations reinforce the importance of selecting tolerant strains and optimizing cultivation conditions (Fadhil et al., 2023; Fadhil et al., 2024). Currently, algae are widely used in various industrial fields (Salman et al., 2025). In addition to their use as a source of food and nutritional supplements for a healthy diet, and in the cosmetics and pharmaceutical industries, they are essential in the production of third-generation ethanol and biodiesel without competing with traditional food crops (Wolkers et al., 2011; Hoyer et al., 2018).

Algae are characterized by their high capacity to convert carbon dioxide and solar energy into lipid-rich biomass, especially microalgae that form colonies, including green algae, which are a complete biological factory due to their chemical richness, making them a

*Correspondence: Mohanad Yakdhan Saleh
E-mail: mohanadalallaf@uomosul.edu.iq

DOI: https://doi.org/10.22034/ijab.v14i3.2909

general source for biorefinery. They contain 30% lipids and 50-70% proteins, and are rich in chemicals such as amino acids, carotenoids, phenols, and sugars, which are used in the production of biofuels and bioplastics (Abd El-Baky and El-Baroty, 2013; Ariede et al., 2017; Avragyan, 2018).

Green algae (Chlorophyceae) are characterized by high cell density and rapid growth (Hawrot-Paw et al., 2020). Methods for culturing them in open or closed reactors have been developed (Bhatia et al., 2021). Alongside conventional cultivation strategies, microscale engineering platforms have broadened the study of biological systems under highly controlled conditions. Microfluidic devices can generate gradients, dynamic microenvironments, and acoustically driven flow fields that enable researchers to examine cell behavior, transport phenomena, and culture responses with high precision. These approaches have become valuable experimental tools in biotechnology and bioengineering research (Al-Abboodi et al., 2011, 2012; Alhasan et al., 2013).

Algae have the ability to produce and concentrate lipids in their cells to a large extent and can be converted into biofuel using various enzymatic, alkaline, and acidic catalysts in esterification reactions more than vegetable seed oils at a ratio of 20-30% (Zhang et al., 2021; Zhu et al., 2023). They also contain polyunsaturated fatty acids such as linoleic acid and stearic acid, reaching tens of percent (Řezanka et al., 2008; Yaseen et al., 2023). The percentage of fatty acid methyl esters in microalgae exceeded 60-80% (Pikoli et al., 2019). In addition, algae are a promising source of starch, achieving up to ten times the productivity of plants (Vilpoux et al., 2023). This starch is used to produce biodegradable bioplastics as an alternative to synthetic plastics made from petroleum polymers (Salah et al., 2021). Microalgae starch is a vital component that can be extracted from carbohydrates stored within algal cells under stress and feeding conditions (Di Caprio et al., 2024).

The genus *Monoraphidium* is a green alga that grows in freshwater environments such as small ponds and lakes, but is generally not widespread. Recent studies have shown that this alga is tolerant and adaptable to low and moderate temperatures and, in turn, yields a high percentage of unsaturated fatty acids, including 10.4% linolenic acid, 32% oleic acid, and palmitic acid. It is a promising candidate for the production of neutral fats and polyhydroxyalkanoates (PHAs), which are raw materials for biofuels, due to its high capacity to accumulate alkanes in its cells (Bogen et al., 2013; Zhao et al., 2014; Georgiou et al., 2024). Their strains are also an important source of starch polymers stored in plastids. The starch granules are distributed in a scattered manner around the pyronoid within the stroma, thereby increasing its ability to store lipids (Fawley et al., 2006). Starch consists of amylose and amylopectin polymers linked by strong internal hydrogen bonds, giving it a semi-crystalline, brittle structure that reacts with glycerol during the manufacture of bioplastics (Wong et al., 2021; Ali et al., 2023). Therefore, this study was conducted to collect and identify *Monoraphidium contortum* from local water bodies in Mosul, Iraq, using morphological and molecular characteristics. Furthermore, after cultivation in multiple media (modified NPK and modified CH10) and exposure to saline stress, lipid transformation and starch valorization were estimated to support the integrated production of biodiesel and bioplastics.

Materials and Methods

Sampling and morphological identification: The sample was collected from the fish-rearing tank in the Department of Biology research laboratory at the College of Education for Pure Sciences, University of Mosul. After confirming the sample's purity, the algae were morphologically identified by preparing temporary slides and examining them under a light microscope at 40X magnification, following Adhabi et al. (2014).

Molecular identification: DNA was extracted using the yeast kit (Promega, M7822) according to the company's protocol. Briefly, in a 1.5 mL Eppendorf microcentrifuge tube, 600 µL of GT buffer was added to the algal cells, and the cells were lysed by vortexing. They were then transferred to a bead-

Table 1. Primers used in PCR reactions.

Primer set	Sequence (5'-3')	Region of amplification
Euk A	AACCTGGTTGATCCTGCCAGT	18srRNA gene
Euk B	TGATCCTTCTGCAGGTTCACCTAC	
P45	ACCTGGTTGATCCTGCCAGT	Microalgal
P47	TCTCAGGCTCCCTCTCCGGA	18srRNA gene

beating tube, with the addition of 5 µL of RNase at 50 mg/mL, and vortexed for 10 minutes at room temperature. The tubes were incubated at 70°C for 10 minutes. During incubation, the tubes were inverted every 3 minutes, then 100 µL of PR solution was added with brief mixing to remove any impurities and resulting foam. The tubes were then incubated on ice for 5 minutes. Afterward, the tubes were centrifuged at 11,000 rpm for 3 minutes at room temperature, and 450 µL of the supernatant was transferred to a new 1.5 mL centrifuge tube. Then 450 µL of GB solution and 450 mL of absolute ethanol were added to the sample, and the mixture was shaken for 10 seconds. The GD column was placed in a 2 mL collection tube, and 700 mL of the sample mixture was transferred to the GD column and centrifuged at 16,000 rpm for 1 minute. Discard the liquid and repeat this process twice. The process continues by adding 400 µL of solution W1 to column GD, centrifuging for 30 seconds at room temperature, and discarding the supernatant. Then, 600 µL of wash buffer was added to the separation column, and the column was centrifuged again to dry the column material. The GD column was fixed in a 1.5 mL tube, and 100 µL of the previously heated elution solution was added and left for 3 minutes to allow binding to DNA. Centrifugation was then performed at 16,000 rpm for 2 minutes at room temperature to extract the purified DNA, which was then stored for use (Hanum et al., 2018).

DNA electrophoresis was used to detect and verify the integrity of DNA bundles in agarose gel. For the preparation of agarose gel, 1 g of agarose powder was added to 100 mL of buffer solution (TAE 1X), heated in the microwave until completely melted, then cooled slightly, and afterward, 3 µL of the safe stain was added while stirring in a circular motion to ensure homogeneity with the dissolved agarose. The mixture was poured into the special tray containing the combs to form the wells and allowed to harden. The tray was then transferred to the buffer solution by removing the combs. Seven µL of the DNA sample was mixed with 3 µL of loading dye in an Eppendorf tube, and 10 µL of the mixture was injected into the wells on the gel surface. The electrophoresis voltage was set to 100 volts for approximately one hour. After the transfer process is complete, the gel is placed under a UV light to visualize the fluorescent DNA bands.

The molecular diagnosis of algae was based on the 18S rRNA region. This region was amplified by adding 3 µL of template DNA and 1 µL of each gene-specific primer (Table 1) to the prepared Master Mix. The samples were thoroughly mixed to prepare them for PCR amplification (Al-Thakafy et al., 2024). The PCR products were sent for sequencing, and the sequences were read using a Genetic Analyzer 3130 (Hitachi, Japan). The algal sequences were matched with gene sequences documented in the NCBI (National Center for Biotechnology Information) BLAST database (Rai et al., 2011).

Preparation of the modified liquid medium (Chu10) for algal growth: The medium was prepared by dissolving the components shown in Table 2 in distilled water, measuring the pH of the medium (7.6-7.8) using a pH meter, and adjusting it with dilute hydrochloric acid (0.1N) and dilute sodium hydroxide (0.1N) (Al-Katib et al., 2017). The medium was then distributed into 1-liter and 250 mL glass containers (Fig. 1) and sterilized in an autoclave at 121°C and 1 atmosphere for 20 minutes (Bold et al., 1985).

Preparation of new culture media: The algae were cultured in multiple media (modified NPK and modified CH10). Medium M1 (NPK 15:15:30) was prepared by dissolving 5 g in 1 L of distilled water, and the pH was adjusted to match the specifications of

Table 2. Components are used to prepare the modified liquid medium for algae culture.

NO.	Compound	Quantity (g/L)
1	K_2HPO_4	0.1
2	Na_2Co_3	0.2
3	$(Ca\ (No_3)_2)$	0.4
4	$MgSo_4.7H_2O$	0.25
5	Ammonium ferric citrate	0.05
6	Na_2Sio_3	0.25

Figure 1. Culture Media of *Monoraphidium contortum*.

the standard medium. Medium M2 (NPK 40:6:13) was prepared by dissolving 5 g in 1 L of distilled water, and the pH was adjusted to match the specifications of the standard medium. Medium M3 (NPK 20:20:20) was prepared by dissolving 5 g in 1 liter of distilled water and adjusting the pH to match the standard medium specifications. Medium M4 ($CaCO_3$ + (NPK 20:20:20) + Chu 10^-) was prepared by adding 5 g/L NPK instead of calcium nitrate, $CaNO_3$, in Chu 10 medium, with the addition of 0.5 g/L calcium carbonate, $CaCO_3$, as a source of calcium. Medium M5 (MgO + (NPK 20:20:20)) was prepared by adding 5 g/L of NPK with the addition of 0.03 g/L of MgO. Medium M6 ($CaCO_3$ + (NPK 20:20:20) was prepared by adding 5 g/L of NPK along with 0.5 g/L of calcium carbonate ($CaCO_3$). Medium M7 (salt stress) was prepared by adding 11 g/L NaCl salt to the modified liquid Chu10 medium.

Algae were grown in Chu10 media for 10-14 days. The ambient conditions were a temperature of 25°C and a photoperiod of 16:8 (light: dark) (Vasumathi et al., 2012). When nutrients were depleted, the biomass was harvested by centrifugation. The biomass was suspended in a saline medium containing NaCl and left to stand for 2-7 days under controlled light and temperature conditions (El-Sheekh et al., 2024). All media were tested in three replicates, and the average was calculated for each medium.

Estimation of algae growth in prepared media: Growth was measured at 3, 7, 10, 12, and 14 days using a spectrophotometer by determining the optical density at 650 nm.

Crude hexane extract of the alga and estimation of oil yield: After collection and sedimentation by centrifugation at 3000 rpm for 10 minutes, the algal sample was oven-dried at 40-50°C for 3-4 days. The samples were ground using an electric grinder and a small ceramic mortar. The dried algae powder was placed in a Whatman (type 1) filter paper thimble in a Soxhlet apparatus according to Verawaty et al. (2017), Karmakar et al. (2018), and Ali et al. (2025). Briefly, 50 grams of dried algal powder are placed in the filter, and 500 mL of hexane is added. After leaving the sample immersed in the solvent for 24 hours, the Soxhlet apparatus was operated at 55°C, and the sample lipid was extracted for 29 hours. The extracted

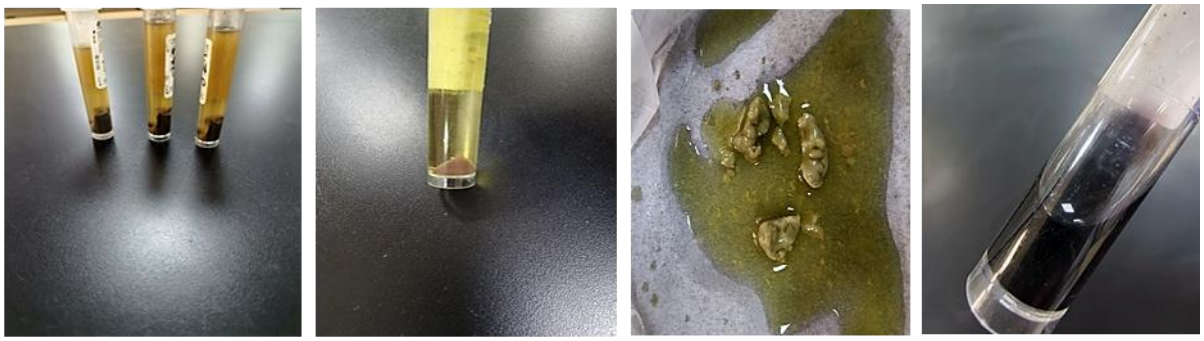

Figure 2. Pictorial stages of starch extraction.

product was transferred to a rotary evaporator to reduce the solvent volume. The resulting oil is placed in a small, airtight container for later use in biodiesel production. The oil yield percentage was estimated by calculating the weight of the algal powder and the weight of the oil (Ozioko, 2012).

Starch extraction from algae: Algae powder used for oil extraction was dried for starch extraction. Two grams of algal powder were dissolved in 20 ml of dimethyl sulfoxide (DMSO) and subjected to ultrasonic treatment for 1 hour at 40-60°C to break down the cell walls. The resulting suspension was then centrifuged at 3000 rpm for 10 minutes. The filtrate was taken to a new evaporator, 1 ml was transferred, and 3 ml of 96% acetone was added to precipitate the sugars. For glucose precipitation only, 96% ethanol (3 mL) was added instead of acetone. The mixture was left to stand for 10 minutes and centrifuged at 5000 rpm for 15 minutes. The precipitate was collected and dried, and the presence of starch was detected with a starch reagent. It was then collected for plastic preparation (Abdallah, 2023; Di Caprio et al., 2024) (Fig. 2).

Characterization of extracted sugar types using high-performance liquid chromatography (HPLC): The extracted sugars were characterized using a German-made SYKAMN HPLC system at the University of Technology/Baghdad, equipped with a C18-NH analytical column (5, 4.5mm × 250mm) for analysis. The sample volume was achieved at 100 microliters, and using the refractive index (RI) detector, the mobile phase composition was (methanol: distilled water) (MeOH: D.W) in a ratio of 98:2, and the flow time was 0.7 ml/ min. (Sesta, 2006).

Preparation of the enriched bioplastic from algal starch: Extracted and dried starch was used by dissolving 2 g of starch in 12.5 ml of distilled water and heating to 90°C with stirring for 10 minutes. Then, 1 ml of acetic acid was added while stirring continuously, and the temperature was reduced to 40°C for 10 minutes. Finally, 1.5 ml of glycerin was added to the mixture as a plasticizer. The mixture was left to stand for 20 minutes, then poured into a Petri dish and dried at room temperature for 4 days (Di Caprio et al., 2024).

Biodegradation test of plastic films in soil: The membranes were examined by burying them in moist soil. The samples were placed in containers filled with sterile sandy soil, moistened with distilled water, and buried at a depth of 12 cm. The initial weight was measured before burial, and then at 15, 40, 70, and 120 days after the soil had dried and the dirt and debris had been removed from the samples. The percentage of weight loss was calculated using the equation weight loss% = ((Mo-M_2)/Mo) x 100% (Hii et al., 2016).

Transesterification process for biodiesel production: 100 mL of extracted oil was mixed with 37 mL of methanol and 2 mL of sulfuric acid (H_2SO_4). The mixture was placed in an ultrasonic device and heated at 40-50°C for 60 minutes to accelerate the reaction. The initial step involved converting free acids. The resulting product was then separated using a separating funnel, and the top layer was collected. To this, 25 mL of methanol and 0.9 g of KOH were added, and the mixture was heated to 60°C. The resulting product was then placed in a separating flask

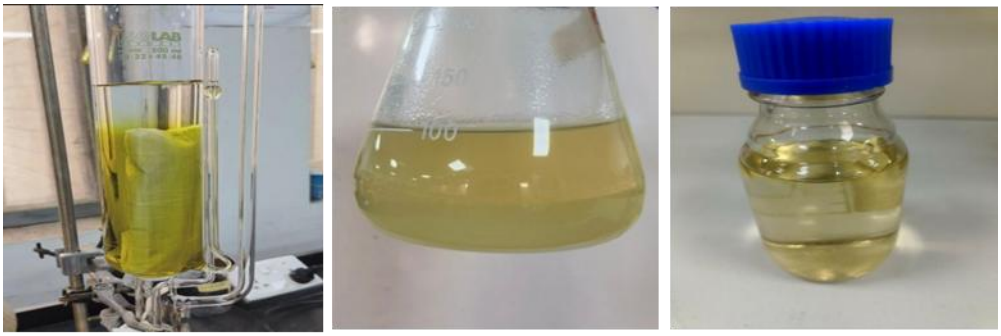

Figure 3. Pictorial stages of biodiesel extraction.

and left for 30-60 minutes to allow the substances to separate. The top layer was biodiesel, and the bottom layer was glycerin. (Hassani et al., 2013; Zhang et al., 2016) (Fig. 3).

Biodiesel purification: Diesel was purified of glycerin and other impurities by washing with a warm 10% water solution at 50°C. Water was gradually added to the biodiesel in the separation funnel, and the process was repeated several times until clear water formed at the bottom of the funnel (Atadashi et al., 2012).

Identification of algal oil components using gas chromatography-mass spectrometry (GC-MS): For this purpose, GC-MS was used, and fatty acids were diagnosed using the same method after the esterification process and preparation of biodiesel in the Central Laboratory, College of Applied Sciences, Samarra University, using a Japanese-made Shimadzu (GC-MS-QP2010 Plus). 40 microliters of algal oil were taken and diluted to 5 ml of ethanol. The instrument's injector was set to 2 µL of the diluted sample using a 30-meter capillary column (Inert Cap 1, a non-polar column bonded with 100% dimethyl polysiloxane) with helium as the carrier gas at a flow rate of 14.5 mL/min. The oven's thermal program was started at 60°C with a 2:1 fractionation ratio, and this temperature was maintained for two minutes. The temperature was increased by 30°C per minute to 180°C, then held for 3 minutes. Afterward, the temperature was increased to 220°C and held for four minutes, with a total holding time of 18 minutes. Mass spectra were recorded over the range 50-900 m/z at an energy of 72 eV. The chemical compounds extracted from the sample were identified by comparing the resulting mass spectra with those in the instrument's software libraries (Hübschmann, 2025).

Fourier transform infrared spectroscopy: The properties of algal oil and biodiesel were analyzed at the Central Laboratory of the College of Science, University of Mosul, using a Bruker FTIR spectrometer.

Statistical analysis: A two-way analysis of variance was used to evaluate the effects of medium type, time, and their interaction, with Tukey's HSD test for comparisons. Statistical analysis of these results was performed using IBM SPSS Statistics (Version 27.0.1),

Results and Discussions

Morphological identification: The pure isolate was identified under a light microscope and, based on its characteristics, is the green alga Monoraphidium contortum, with single, curved, arched cells and a pyrenoid chloroplast (John et al., 2002; Lee, 2018) (Fig. 4).

Molecular identification: Based on the results, the isolate belongs to the microgreen algae of *Monoraphidium contortum*. with a match of 84%. The length of the recorded gene was 1218 base pairs, and it was stored in GenBank with accession number MH203022. Although this ratio appears lower than typical species-level concordance, it indicates evolutionary divergence and distinct variation in this locally isolated sample within Iraqi environments. When compared with published global isolates, this isolate showed a high degree of similarity, confirming

Table 3. Optical Density measurements at 650 nm.

Media \ Days	3	7	10	12	14
Chu10	0.339^{bC}	0.515^{bC}	0.728^{bB}	1.706^{aA}	1.502^{Aa}
M1	0.298^{bcB}	0.391^{cdAB}	0.420^{cdA}	0.568^{dA}	0.314^{cB}
M2	0.231^{cdB}	0.338^{deAB}	0.353^{deAB}	0.485^{deA}	0.292^{cB}
M3	0.220^{dB}	0.334^{deAB}	0.339^{eAB}	0.459^{eA}	0.258^{cB}
M4	0.480^{aC}	0.855^{aB}	1.056^{aB}	1.742^{aA}	0.950^{bB}
M5	0.188^{dB}	0.276^{eAB}	0.363^{deA}	0.420^{eA}	0.223^{cB}
M6	0.298^{bcC}	0.353^{dC}	0.601^{cB}	0.940^{cA}	0.886^{bA}

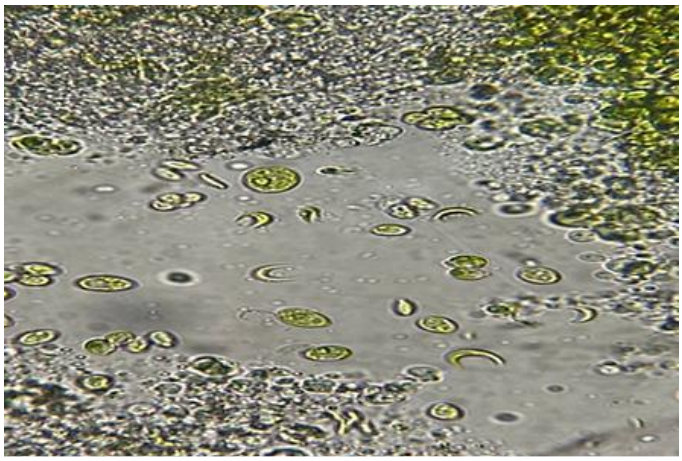

Figure 4. Microscopic image of *Monoraphidium contortum*

the identity of this species.

Estimating algae growth: At 650 nm, absorbance varied among media, with three replicates (n=3) (Table 3). The results revealed a significant difference in the efficacy of the seven-nutrient media on algal growth (P<0.05). The results showed that medium M4 achieved a dominant, early lead starting on the third day and continued to increase, peaking on the twelfth day at an optical density of 1.742. This medium not only outperformed the other media on that day (vertical comparison) but also achieved its maximum biological performance compared to all other time periods (horizontal comparison). This behavior reflects the high efficiency of this medium's components in stimulating the logarithmic growth phase (Log Phase), making it the optimal medium for rapid biomass production. In contrast, on the 14th day, an important biological phenomenon emerged: medium M4 showed a sharp, significant decline, while medium Chu10 remained stable at 1.502. This discrepancy indicates that the explosive growth stimulated by medium M4 led to the rapid depletion of essential nutrients or the accumulation of secondary metabolic products (Dumas et al., 1998), thereby accelerating the cells' entry into the decline phase. Meanwhile, the Chu10 medium proved to be the most sustainable for long-term cultures. The M6 medium showed stable, increasing growth that was superior to that of M1, M2, M3, and M5 (Fig. 5).

Estimation of oil yield: The amount of oil was 4.8g/50g dry weight of the algae, indicating a yield of 9.6% (Table 4). The results showed that oil extraction increased by 9.6% under salinity stress. Although the increase was not high and did not differ significantly, salinity stress acted as a biochemical modifier in increasing the production of polyunsaturated fatty acids, which are of industrial importance for biodiesel in improving its properties in terms of maintaining its fluidity and preventing it from freezing inside engine pipes, especially in cold regions (Knothe, 2005).

Characterization of the extracted sugar types: The results indicate that three types of sugars are extracted from algae: glucose and fructose, at 55.48% and 32.18%, respectively, both of which are monosaccharides, and sucrose at 12.34%, which is a disaccharide. Glucose had the highest percentage among the components (Fig. 6).

Assessment of plastic biodegradation: The biodegradation results for plastic manufactured from algal starch showed a high capacity for decomposition in moist soil (Table 5, Fig. 7-8). The plastic lost 0.390 grams over 15, 40, 70, and 120 days. The preliminary stage (lag phase) lasted 15 days, during which the decomposition rate reached 8.97%, with a daily average of 0.58 grams. The sample gradually lost its transparency, turned a distinct color, and developed slight wrinkles on its surface. This is because

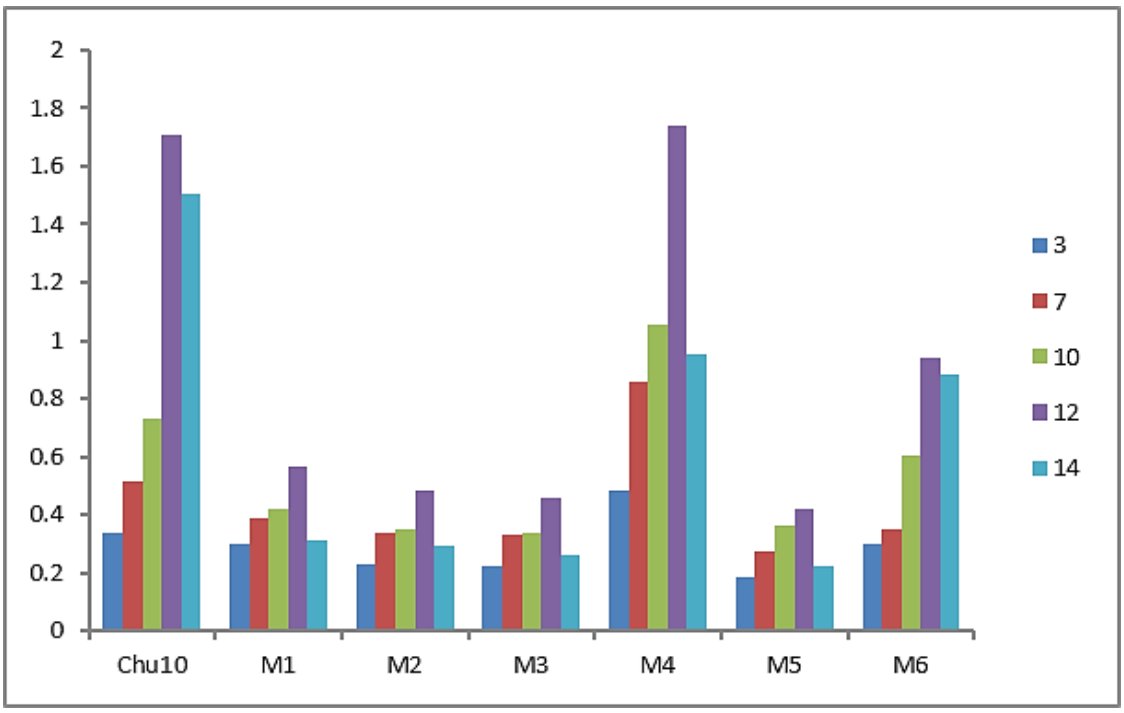

Figure 5. Variation in algal growth density across various cultivation media.

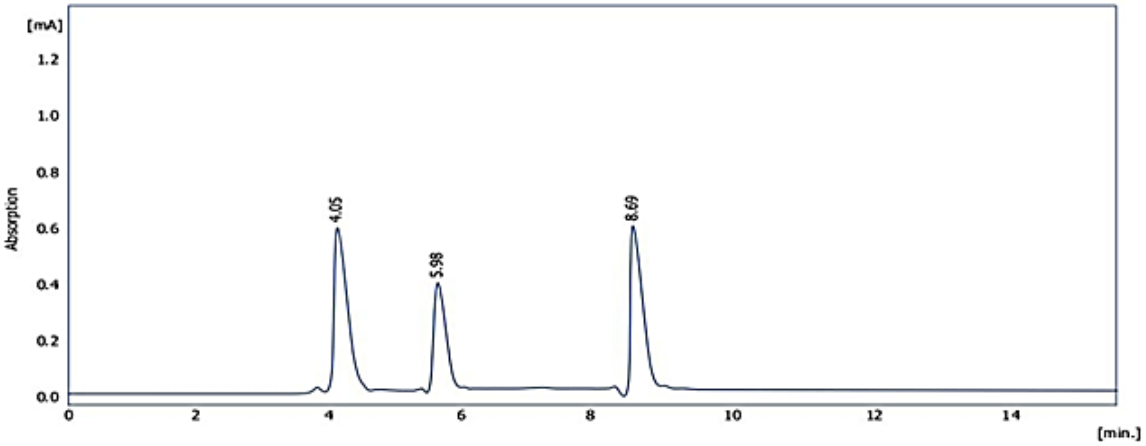

Result chromatography Table (Uncal - F:\ sample 4)

No	Reten. Time [min]	Area [mAU.s]	Height [mAU]	Area [%]	Height [%]	W05 [min]	Compound Name
1	4.05	6589.70	587.47	35.00	35.00	0.15	
2	5.98	4122.05	388.59	30.00	30.00	0.10	
3	8.69	7011.98	590.14	35.00	35.00	0.15	
	Total	17723.49	1566.20	100.00	100.00		

Figure 6. The results of the HPLC analysis of algal sugar.

microorganisms need a period to adapt to the polymer surface. The second stage, the active accelerated decomposition phase, was characterized by a significant acceleration in the decomposition process and a weight loss of 23.5 to 62.8%, with a daily average of 1.30%. This indicates the decomposition process and the breaking of polymer chains in the sample due to increased moisture content and the reaction between water and hydrogen bonds (Doh, 2021), as well as the action of enzymes and microorganisms, which led to the appearance of small holes. The sample broke easily upon touch, and at 70 days it began to break into small, fragmented pieces, consistent with previous findings (Dudek and Coskun, 2017; Khalil et al., 2017). On day 120, the stabilization phase began, during which the decomposition rate reached 68.2%, and the sample became microfibers integrated into the soil. This slower decomposition is

Table 4. Estimation of oil yield in *Monoraphidium contortum*.

Weight before extraction (g)	Weight after extraction (g)	Time(hours)	Oil Weight (g)	Yield (%)	Starch Weight
50g	45g	29h	4.8 g	9.6%	1.25g

Table 5. Biodegradation stages of bioplastic in soil.

Time (days)	Weight(g)	Weight loss
0	0.390	0
15	0.355	8.97
40	0.298	23.59
70	0.145	62.82
120	0.124	68.20

due to the retention of more complex parts of the polymer structure, which require more enzymatic energy to break down (Sharma et al., 2020). This high decomposition rate over 120 days meets the international standards (ASTM D6400) for classifying biodegradable polymers. The decomposition rate of 68.2% exceeded the international standard decomposition rate of 60%. This confirms the efficiency of algae-based plastic as an alternative to traditional plastics, its environmental friendliness, and its high potential for integration into the natural carbon cycle (Al-Sultan et al., 2022).

Effect of salt stress on algal oils and conversion to biodiesel: GC-MS analysis of the oil showed clear chemical transformation of lipids between algal growth in Chu10 medium and salt-stressed medium (M7). This demonstrated the effectiveness of salt stress in modifying lipid composition, thereby influencing the success of the stereotypes (Thamer and Saleh, 2026). The algal oil sample growing in Chu10 medium exhibited a standard distribution of saturated fatty acids and long-chain alkanes (C14-C18), representing the basic metabolic state of the algae (Fig. 9). The presence of heptadecane and undecane compounds is consistent with previously reported hydrocarbon synthesis in algae, and these compounds contribute to the formation of hydrophobic barriers and are associated with the vegetative growth of the alga. This is consistent with the results of Ramos et al. (2009) and Saleh et al. (2022). In addition to the notable and special presence of cis vaccenic acid, which is a monounsaturated fatty acid and an antioxidant derivative of lovable (1-(+)-

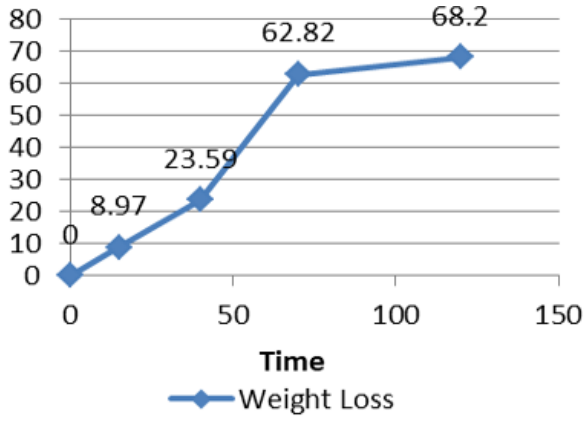

Figure 7. The results of the biodegradation curve of the synthesized bioplastic in soil.

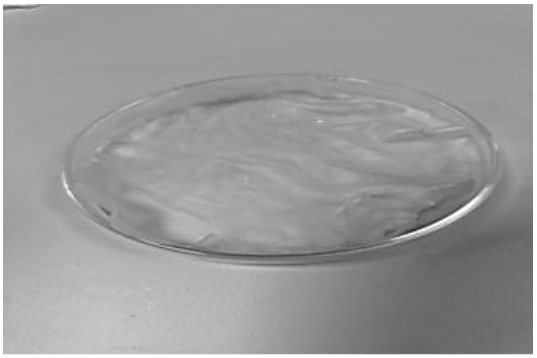

Bioplastic image before burial

Bioplastic image after burial

Figure 8. The pictorial results of bioplastic degradation.

Ascorbic acid 2,6-dihexadecanoate), the compound was determined to be relatively abundant in lipids and may contribute to the oxidative stability of the oil fraction, and indicates the presence of internal antioxidant defense mechanisms in algae. This shows

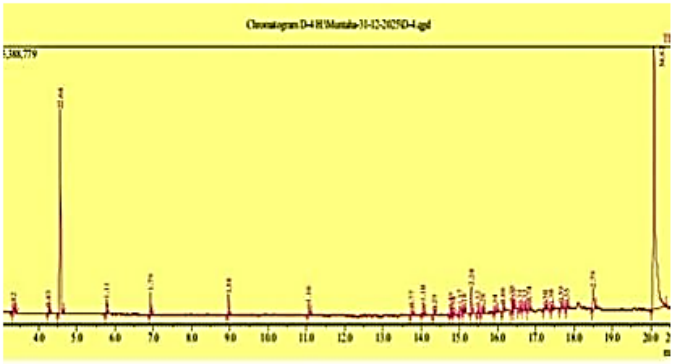

Peak Report TIC

Area%	Height	Height%	A/H	Name
7.41	285666	11.73	1.09	Tetraethyl silicate
7.33	178041	7.31	1.73	Undecane
0.91	6932	0.28	5.52	16-Hexadecanoyl hydrazide
0.86	18233	0.75	1.97	Undecane, 3-methyl-
18.79	642407	26.38	1.23	Dodecane
0.88	5276	0.22	6.99	Hydrazinecarboxamide
1.38	5718	0.23	10.12	Acetic acid, hydrazide
1.31	18823	0.77	2.92	Tridecane, 2-methyl-
17.88	514543	21.13	1.46	Tetradecane
1.92	40046	1.64	2.02	2-((2-Butoxyethoxy)carbonyl)benzoic acid
9.28	214088	8.79	1.82	Hexadecane
1.10	19596	0.80	2.36	Nonane, 3-methyl-5-propyl-
1.20	15656	0.64	3.22	Hydrazinecarboxamide
5.47	146217	6.00	1.57	Heptadecane
10.45	166342	6.83	2.64	l-(+)-Ascorbic acid 2,6-dihexadecanoate
1.04	23438	0.96	1.86	Hexadecanoic acid, ethyl ester
2.68	54308	2.23	2.07	Eicosane
1.59	14546	0.60	4.59	Diisooctyl phthalate
5.17	31806	1.31	6.83	Diisooctyl adipate
3.37	33560	1.38	4.21	cis-Vaccenic acid
100.00	2435242	100.00		

GC-MS results for algae oil grown in Chu10 medium

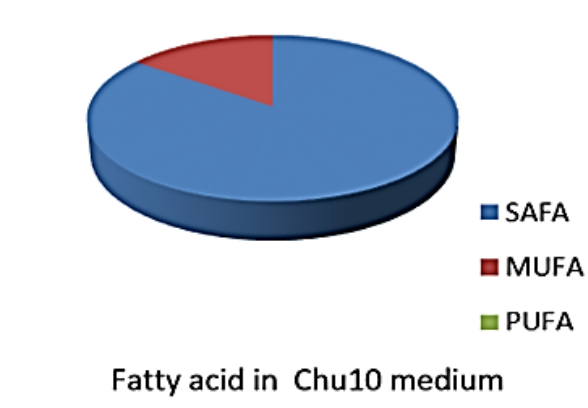

Fatty acid in Chu10 medium

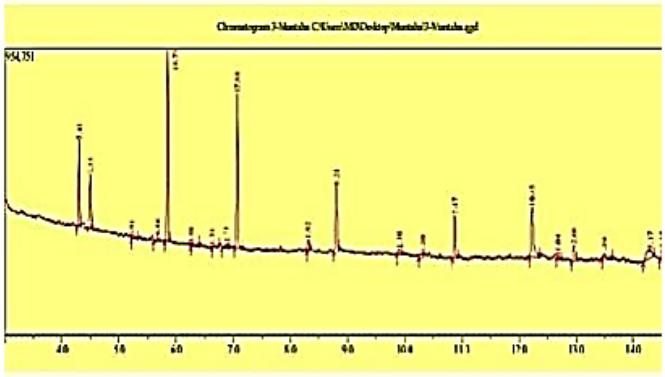

Peak Report TIC

Area%	Height	Height%	A/H	Name
0.82	69485	0.51	4.13	Nonane
0.43	117405	0.86	1.26	Tetraethyl silicate
22.64	3948473	29.01	2.00	Undecane
1.11	280068	2.06	1.37	Undecane
1.79	458735	3.37	1.35	Dodecane
1.58	412006	3.03	1.33	Tetradecane
1.16	233144	1.71	1.73	Hexadecane
0.77	170248	1.25	1.58	Heptadecane
1.10	247031	1.82	1.55	2-Pentadecanone, 6,10,14-trimethyl-
0.29	66870	0.49	1.51	Cyclononasiloxane, octadecamethyl-
0.49	113305	0.83	1.52	Hexadecanoic acid, methyl ester
0.34	49328	0.36	2.37	Dibutyl phthalate
1.37	171475	1.26	2.78	l-(+)-Ascorbic acid 2,6-dihexadecanoate
0.18	41410	0.30	1.48	Ethyl 9-hexadecenoate
2.24	522820	3.84	1.49	Hexadecanoic acid, ethyl ester
0.52	124847	0.92	1.44	Heneicosane
0.28	63521	0.47	1.51	Cyclodecasiloxane, eicosamethyl-
0.34	36324	0.27	3.25	n-Tetracosanol-1
0.66	149314	1.10	1.54	Phytol
0.75	160543	1.18	1.62	9,12-Octadecadienoic acid, ethyl ester
0.35	85268	0.63	1.43	9-Octadecenoic acid, ethyl ester
0.39	72649	0.53	1.89	Cyclooctasiloxane, hexadecamethyl-
0.33	78257	0.58	1.48	Heneicosane
0.74	144344	1.06	1.78	Tributyl acetylcitrate
0.50	51332	0.38	3.42	2-methylhexacosane
0.30	63262	0.46	1.65	Cyclononasiloxane, octadecamethyl-
0.59	101709	0.75	2.03	Diisooctyl adipate
0.35	61222	0.45	1.97	Eicosane
2.79	413443	3.04	2.35	Diisooctyl phthalate
54.82	5101835	37.49	3.74	1,4-Benzenedicarboxylic acid, bis(2-ethylhexy
100.00	13609673	100.00		

GC-MS results for algae oil in a saline stress medium

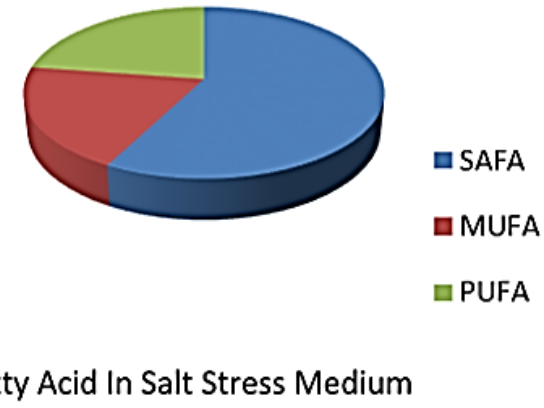

Fatty Acid In Salt Stress Medium

Figure 9. The results of fatty acid composition of algal oil according to growth media.

that the percentage of saturated fatty acids (SFA) is 85.1%, monounsaturated fatty acids (MUFA) is 14.9%, and there are no polyunsaturated fatty acids (PUFA).

The GC-MS results showed that the algal salt stress phase led to the stimulation and accumulation of lipids as a defensive response to osmotic pressure (Fig. 9). This phase was characterized by a change in the

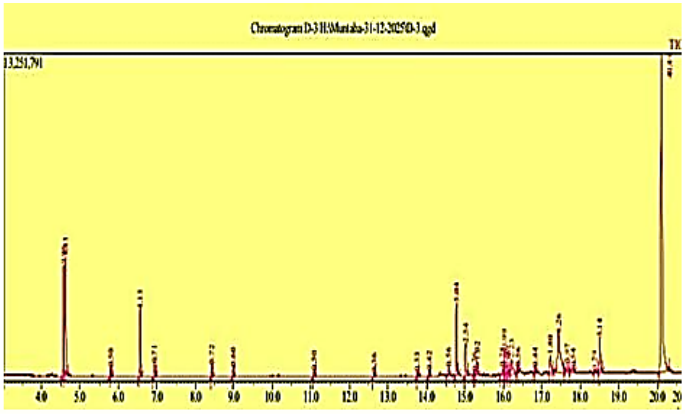

Peak Report TIC

Area%	Height	Height%	A/H	Name
9.96	4494814	11.19	1.99	Undecane
8.83	4829530	12.03	1.64	Cyclotetrasiloxane, octamethyl-
0.50	344734	0.86	1.30	Undecane
4.13	2716256	6.76	1.37	Cyclopentasiloxane, decamethyl-
0.71	502604	1.25	1.27	Dodecane
0.72	499671	1.24	1.29	Cyclohexasiloxane, dodecamethyl-
0.60	406469	1.01	1.34	Tetradecane
0.50	253292	0.63	1.77	Hexadecane
0.36	165514	0.41	1.96	Methyl tetradecanoate
0.33	190937	0.48	1.53	Heptadecane
0.42	248710	0.62	1.53	2-Pentadecanone, 6,10,14-trimethyl-
0.56	311298	0.78	1.63	11-Hexadecenoic acid, methyl ester
5.04	2956441	7.36	1.53	Hexadecanoic acid, methyl ester
2.54	1336275	3.33	1.71	l-(+)-Ascorbic acid 2,6-dihexadecanoate
0.26	172715	0.43	1.36	2,3-Dimethyl-undec-1-en-3-ol
1.02	576725	1.44	1.58	Hexadecanoic acid, ethyl ester
0.78	326282	0.81	2.16	10,13-Octadecadienoic acid, methyl ester
1.99	1080779	2.69	1.65	cis-13-Octadecenoic acid, methyl ester
1.06	355778	0.89	2.68	2-Dodecenal
0.56	164492	0.41	3.04	Phytol
2.23	609339	1.52	3.28	10-Octadecenoic acid, methyl ester
0.56	253001	0.63	1.99	Z,Z-8,10-Hexadecadien-1-ol
0.44	243981	0.61	1.61	Tributyl acetylcitrate
1.80	690824	1.72	2.35	9-Octadecenoic acid, 12-hydroxy-
8.26	1563359	3.89	4.74	1,4-Benzenedicarboxylic acid, bis(2-ethylhexy
0.97	323955	0.81	2.69	Hexanedioic acid, bis(2-ethylhexyl) ester
0.54	159776	0.40	3.06	4'-(Trifluoromethyl)acetophenone
0.29	71954	0.18	3.66	Oxalic acid, 2-ethylhexyl pentadecyl ester
3.14	1396057	3.48	2.02	Diisooctyl phthalate
40.89	12915477	32.16	2.84	1,4-Benzenedicarboxylic acid, bis(2-ethylhexy
100.00	40161039	100.00		

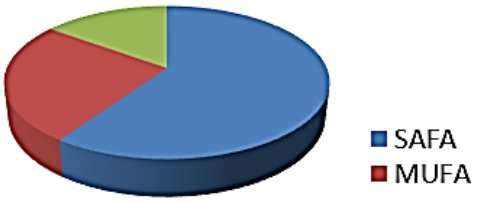

Fatty acid in biodiesel

Figure 10. The results of GC–MS of biodiesel composition and fatty acid ratios.

proportions of fatty acids, including 9,12-octadecadenoic acid, ethyl ester, of which saturated fatty acids constituted 57.7% and monounsaturated fatty acids 19.6%. Stress decreased saturated fatty acids and increased polyunsaturated fatty acids by 22.7%. Following this, the algae carried out a biological defense chemical transformation, altering their cellular fluidity. An increase in the percentage of the compound Phytol was observed, which is considered a chemical signature and an indicator of the algal cells' response to intercellular stress (Pan et al., 2024).

The results showed successful conversion of crude algal oil into biodiesel, with fatty acids present as esters (Fig. 10). This is evidence of the success of the reaction process (10-octadecenoic acid, methyl ester (Saeed et al., 2025). Transesterification is the best way to reduce viscosity and convert algal oils into fuel that conforms to specifications and standards (ASTM D6751). The results showed that the percentages of saturated, monounsaturated, and polyunsaturated fatty acids were 59.6, 25.4, and 15.0%, respectively. The presence of hydroxyl acids, such as 9-octadecenoic acid and 12-hydroxy-9, was observed. These compounds increase fuel efficiency and improve engine lubricity, thereby reducing mechanical friction (Hao et al., 2025).

Analysis of algal oil and biodiesel using infrared spectroscopy: The results show the chemical characteristics of the triglycerides in crude oil, where the peak at 1730 cm^{-1} represents the carbonyl group C=O of the ester in the triglycerides, the peak between 2850-2930 cm^{-1} represents the stretching vibrations in the long fatty acid chains, and the CH_2 and CH_3 groups are very strong groups, indicating a high hydrocarbon content (Fig. 11) (Saleh et al., 2025). A peak was also observed between 1000-1460 cm^{-1}, which is the fingerprint region, corresponding to methylene group vibrations and representing the characteristic pattern of crude algal oil.

The FTIR results showed key distinctive changes confirming the esterification process (Fig. 12). The carbonyl (C=O) peak at 1728 cm^{-1} in biodiesel (methyl esters) was more pronounced and intense than in crude oil. The spectral results showed new peaks at 1100-1300 cm^{-1} due to the extension of C-O bonds in methyl esters, a distinguishing feature between biodiesel and crude oil, which agrees with the findings of Husar et al. (2025). A stable section was observed between 2859 -2923 cm^{-1}, a strong peak indicating the stability of the hydrocarbon peak and that the chains were not affected; only the terminal groups changed to monoesters instead of triglycerides. The absence of

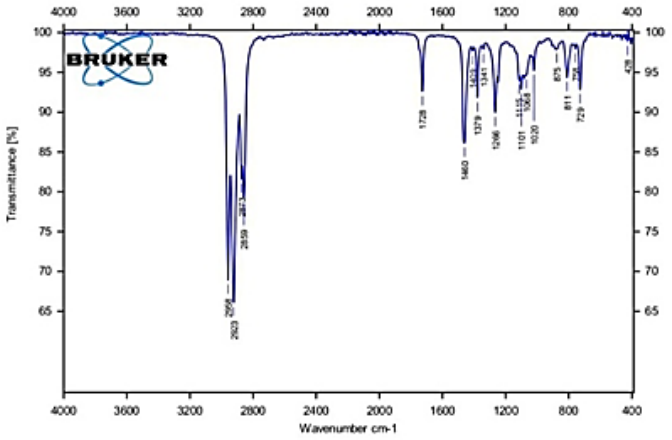

Figure 11. The results of FTIR of crude oil produced from *Monoraphidium contortum*.

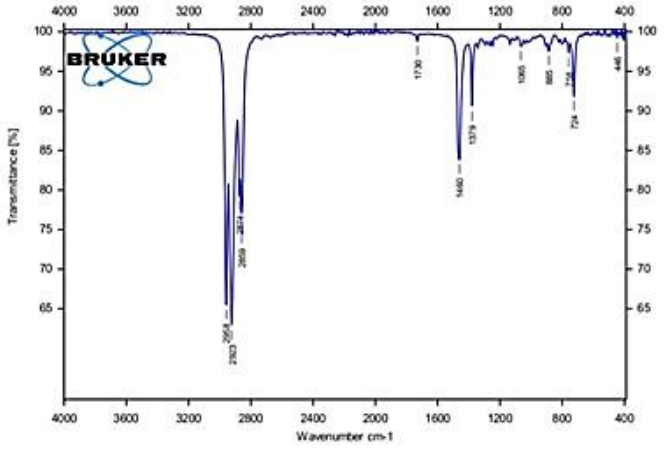

Figure 12. The results of FTIR of biodiesel produced from *Monoraphidium contortum*.

any broad band in the 3400 cm^{-1} region of the diesel indicates the product's quality and freedom from residues of glycerin, water, and unreacted alcohol. This demonstrates the efficiency of the washing and drying process (Saleh and Saleh, 2022).

Conclusion

This study concludes that the alga *M. contortum* represents an ideal model of an integrated biorefinery. The 18S rRNA region results demonstrated high efficiency in identifying the local isolate and provided a robust 1,218-base-pair genetic reference. The study confirmed that exposing the alga to salt stress at 11 g/L is a crucial biochemical strategy for stimulating lipid accumulation and modifying its chemical composition. This stress led to a significant increase in the proportion of polyunsaturated fatty acids (PUFAs), reaching 22.7%, a defensive shift evidenced by the emergence of the compound Phytol as a response signature to the harsh environmental conditions. Regarding the quality of the biofuel, the transesterification process demonstrated technical success in converting crude oil into biodiesel that meets international standards (ASTM D6751). FTIR and GC-MS analyses demonstrated the conversion of fatty acids to methyl esters, with a significant increase in the percentage of monounsaturated fatty acids (MUFAs) in the diesel to 25.4%. This provides an ideal balance between combustion efficiency and fluidity. The study also concluded that the economic value of biomass can be maximized by extracting starch, which contains 55.48% glucose, and converting it into sustainable bioplastics. Finally, the choice of biodegradation provided conclusive evidence of the product's environmental friendliness. The manufactured plastic achieved a decomposition rate of 68.2% within 120 days, exceeding the international standard (ASTM D6400) and confirming its suitability as a bio-based alternative fully integrated into the natural carbon cycle.

Acknowledgment

The authors are grateful to the researchers at the University of Mosul for their support in the field and laboratory works.

References

Abd El Baky H. (2013). Healthy benefit of microalgal bioactive substances. Journal of Aquatic Science, 1(1): 11-23.

Abdallah M.R. (2023). Validation of a modified starch-iodine test for rapid determination of starch content in emulsion luncheon sausage. Assiut Veterinary Medical Journal, 69(179): 237-243.

Adhabi A.M. (2014). Practical phycology. Ministry of Higher Education and Scientific Research, University of Basra, Dar Al-Kutub for Printing and Publishing, University of Basra.

Al-Abboodi A., Tjeung R., Doran P., Yeo L., Friend J., Chan P. (2011). Microfluidic chip containing porous gradient for chemotaxis study. Smart Nano-Micro Materials and Devices, 8204: 219-224.

Al-Abboodi A., Tjeung R., Doran P., Friend J., Chan P. (2012). Generation of dynamic microenvironment in a hydrogel-based microfluidic device for cell culture study. Proceedings of the 16th International Conference on Miniaturized Systems for Chemistry and Life Sciences Microtas. pp: 1636-1638.

Alhasan L., Qi A., Al-Abboodi A., Rezk A., Shilton R.R., Chan P.P., ... Yeo L. (2013). Surface acoustic streaming in microfluidic system for rapid multicellular tumor spheroids generation. In: Micro/Nano Materials, Devices, and Systems, 8923: 828-831.

Ali A.H., Saleh M.Y., Owaid K.A. (2023). Mild synthesis, characterization, and application of some polythioester polymers catalyzed by cetrimide ionic liquid as a green and eco-friendly phase-transfer catalyst. Iranian Journal of Catalysis, 13(1).

Ali A.H., Saleh M.Y., Yaqoob Q.A., Saied S.M., Hasan M.S., Owaid K.A., Alsirhani A.M. (2025). Comprehensive evaluation of antibacterial and anticancer activities from indole butanoic acid. Journal of Genetic Engineering and Biotechnology, 23(1), 100452.

Al-Katib M.O. (2017). Estimation of acetic acid hormone in some local microalgae and its partial isolation and characterization from green algae *Gloeocapsa* spp. PCC 7428 and studying the production and effect of silver nanoparticles on it. PhD thesis, College of Education, University of Mosul. 189 p.

Al-Sultan R.M.H., Al-Sultan A.A., Hayawi M.A., Aldahham B.J., Saleh M.Y., Mohammed H.A. (2022). The effect of subclinical thyroid dysfunction on B-type natriuretic peptide level. Revis Bionatura, Revista Bionaturam 7(2/21): 99-108.

Al-Thakafy N.T., Abdelzaher M.A., Abdelzaher H.G., Saleh M.Y., Al-Enizzi M.S., Saied S.M., Moghanm F.S. (2024). A novel chalcone compound as a reagent for the validation of pharmaceutical cefotaxime sodium preparations. Results in Chemistry, 7: 101387.

Ariede M.B., Candido T.M., Jacome A.L.M., Velasco M.V.R., de Carvalho J.C.M., Baby A.R. (2017). Cosmetic attributes of algae - A review. Algal Research, 25: 483-487.

Atadashi I.M., Aroua M.K., Abdul Aziz A.R., Sulaiman S.A. (2012). The effect of hot water washing on the removal of impurities from crude biodiesel. Fuel Processing Technology, 95: 143-147.

Avragyan A. (2018). The use of microalgae for biofuel production and need in improvements of global environmental policy. In: Proceeding of 11th world Bioenergy congress and expo, July 2-4, 2018, Berlin, Germany.

Aziz Z.S., Jazza S.H., Dageem H.N., Banoon S.R., Balboul B.A., Abdelzaher M.A. (2024). Bacterial biodegradation of oil-contaminated soil for pollutant abatement contributing to achieve sustainable development goals: A comprehensive review. Results in Engineering, 22: 102083.

Benouis K., Khane Y., Ahmed T., Albukhaty S., Banoon S.R. (2022). Valorization of diatomaceous earth as a sustainable eco-coagulant for wastewater treatment: optimization by response surface methodology. Egyptian Journal of Chemistry, 65(9): 777-788.

Bhatia S.K., Mehariya S., Bhatia R.K., Kumar M., Pugazhendhi A., Awasthi M.K., ... Yang Y.H. (2021). Wastewater based microalgal biorefinery for bioenergy production: Progress and challenges. Science of the Total Environment, 751: 141599.

Bogen C., Klassen V., Wichmann J., La Russa M., Doebbe A., Grundmann M., Mussgnug J.H. (2013). Identification of *Monoraphidium contortum* as a promising species for liquid biofuel production. Bioresource Technology, 133: 622-626.

Bold H.C., Wynne M.J. (1985). Introduction to the algae. Prentice Hall. Inc. New Jersey. 720 p.

Di Caprio F., Pedram N., Brugnoli B., Francolini I., Altimari P., Pagnanelli F. (2024). Exploring different processes for starch extraction from microalgae and synthesis of starch-chitosan plastic films. Bioresource Technology, 413: 131516.

Doh H. (2020). Development of seaweed biodegradable nanocomposite films reinforced with cellulose nanocrystals for food packaging (Doctoral dissertation, Clemson University). 211 p.

Dudek S., Coskun M.C. (2017). Biopolymer Compounds for Applications Requiring Marine Degradation. ANTEC Anaheim. 415 p.

Dumas A., Laliberte G., Lessard P., De La Noüe J. (1998). Biotreatment of fish farm effluents using the cyanobacterium *Phormidium bohneri*. Aquacultural Engineering, 17(1): 57-68.

El-Sheekh M.M., Galal H.R., Mousa A.S.H., Farghl A.A. (2024). Impact of macronutrients and salinity stress on biomass and biochemical constituents in *Monoraphidium braunii* to enhance biodiesel production. Scientific Reports, 14(1): 2725.

Fadhil A.A., Mohammed S.J., Al-Abboodi A. (2023).

Morphological responses of plants to air pollutants: A comparative study on leaf changes in five species. Iranian Journal of Ichthyology, 10: 286-293.

Fadhil A.A., Swaid S.Y., Mohammed S.J., Al-Abboodi A. (2024). Impact of salinity on tomato seedling development: A comparative study of germination and growth dynamics in different cultivars. Journal of Chemical Health Risks, 14(1): 183-190.

Fawley M.W., Dean M.L., Dimmer S.K., Fawley K.P. (2006). Evaluating the morphospecies concept in the Selenastraceae (Chlorophyceae, Chlorophyta). Journal of Phycology, 42(1): 142-154.

Georgiou D., Exarhopoulos S., Charisis A., Simitsis S., Papapanagiotou G., Samara C., ... Kalogianni E.P. (2024). Valorization of *Monoraphidium* sp. microalgal biomass for human nutrition applications. Journal of Applied Phycology, 36(3): 1293-1309.

Hanum L., Windusari Y., Setiawan A., Muharni M., Adriansyah F., Mubarok A.A. (2018). Comparison of CTAB method and wizard genomic DNA purification system kit from Promega on DNA isolation of local varities of rice of South Sumatera. Science and Technology Indonesia, 3(1): 26-29.

Hao Y., Zhang K., Wang J., Wang R., Zhang G., Duan R., Wang X. (2025). Bio-based lubricants: Progress in research. BioResources, 20(3): 8349.

Hassan S.A.D.H., Al Naqeeb N.A., Al-Musawi M.R., Banoon S.R., Mohammed M.K., Bilal M., Abdelzaher M.A. (2025). Using artificial intelligence to predict aquatic pollution: A comprehensive review. International Journal of Aquatic Biology, 13(5): 50-67.

Hassani M., Amini G., Najafpour G.D., Rabiee M. (2013). A two-step catalytic production of biodiesel from waste cooking oil. International Journal of Engineering, 26(6C). 10.5829/idosi.ije.2013.26.06c.01

Hawrot-Paw M., Koniuszy A., Gałczyńska M. (2020). Sustainable production of *Monoraphidium* microalgae biomass as a source of bioenergy. Energies, 13(22), 5975.

Hii S.L., Lim J.Y., Ong W.T., Wong C.L. (2016). Agar from Malaysian red seaweed as potential material for synthesis of bioplastic film. Journal of Engineering Science and Technology, 7: 1-15.

Hoyer J., Cotta F., Diete A., Großmann J. (2018). Bioenergy from Microalgae–Vision or Reality? ChemBioEng Reviews, 5(4): 207-216.

Hübschmann H.J. (2025). Handbook of GC-MS: fundamentals and applications. John Wiley and Sons.735 p.

Husar J., Sanek L., Pecha J. (2025). Real-time FTIR-ATR spectroscopy for monitoring ethanolysis: Spectral evaluation, regression modelling, and molecular insight. International Journal of Molecular Sciences, 26(19): 9381.

IBM Corp. (2020). IBM SPSS Statistics for Windows, Version 27.0. Armonk, NY: IBM Corp.

John D.M., Whitton B.A., Brook A.J. (2002). The freshwater algal flora of the British Isles: An identification guide to freshwater and terrestrial algae. Cambridge University Press. 878 p.

Karmakar R., Rajor A., Kundu K., Kumar N. (2018). Production of biodiesel from unused algal biomass in Punjab, India. Petroleum Science, 15(1): 164-175.

Khalil H.P.S.A., Tye Y.Y., Saurabh C.K., Leh C.P., Lai T. K., Chong E.W.N., Syakir M.I. (2017). Biodegradable polymer films from seaweed polysaccharides: A review on cellulose as a reinforcement material. Express Polymer Letters, 11(4) 244-265.

Knothe G. (2005). Dependence of biodiesel fuel properties on the structure of fatty acid alkyl esters. Fuel Processing Technology, 86(10): 1059-1070.

Lee R.E. (2018). Phycology. Cambridge University Press. 535 p.

Malla F.A., Bandh S.A., Wani S.A., Hoang A.T., Sofi N.A. (2023). Biofuels: Potential alternatives to fossil fuels. In: Biofuels in circular economy. Singapore: Springer Nature Singapore. pp: 1-15.

Ozioko F.U. (2012). Extraction and characterization of soybean oil-based bio-lubricant. AU Journal of Technology, 15(4).

Pan Y., Amenorfenyo D.K., Dong M., Zhang N., Huang X., Li C., Li F. (2024). Effects of salinity on the growth, physiological and biochemical components of microalga *Euchlorocystis marina*. Frontiers in Marine Science, 11: 1402071.

Pikoli M.R., Sari A.F., Solihat N.A., Permana A.H. (2019). Characteristics of tropical freshwater microalgae *Micractinium conductrix*, *Monoraphidium* sp. and *Choricystis parasitica*, and their potency as biodiesel feedstock. Heliyon, 5(12).

Rai M., Duran N. (2011). Metal nanoparticles in microbiology. Springer Science and Business Media. 567 p.

Ramos M.J., Fernández C.M., Casas A., Rodríguez L., Pérez Á. (2009). Influence of fatty acid composition of raw materials on biodiesel properties. Bioresource

Technology, 100(1): 261-268.

Rashid M.K., Salman I.R., Obaid A.L., Hassan S.A.D.H., Al-musaw, M.R., Al-Saady M. (2024). Application of machine learning in predicting sources of water pollution in the Euphrates and Tigris rivers in Iraq. International Journal of Aquatic Biology, 12(6): 581-589.

Řezanka T., Nedbalová L., Sigler K. (2008). Unusual medium-chain polyunsaturated fatty acids from the snow alga *Chloromonas brevispina*. Microbiological Research, 163(4): 373-379.

Saeed N.H., Ali R.T., Saied S.M. (2025). Computational study on the Estramustine (EMCYT) and its active metabolites anticancer drugs 17-α-estradiol and nornitrogen. *Resu*lts in Chemistry, 102747.

Salah H.M., Alkhalidi M.M.A., Abulridha H.A., Banoon S. R., Abdelzaher M.A. (2021). Current situation and future prospects for plastic waste in Maysan governorate: Effects and treatment during the COVID-19 pandemic. Egyptian Journal of Chemistry, 64(8): 4449-4460.

Saleh A., Saleh M.Y. (2022). Synthesis of heterocyclic compounds by cyclization of Schiff bases prepared from capric acid hydrazide and study of biological activity. Egyptian Journal of Chemistry, 65(12): 783-792.

Saleh M.Y., Al-barwari A.S., Ayoob A.I. (2022). Synthesis of some novel 1, 8-naphthyridine chalcones as antibacterial agents. Journal of Nanostructures, 12(3): 598-606.

Saleh M.Y., Aldulaimi A.K.O., Saeed S.M., Adhab A.H. (2025). Palladium fabricated on Fe3O4 as an organic-inorganic hybrid nanocatalyst for the Suzuki and Stille coupling reactions. Journal of Molecular Structure, 1321: 139597.

Salman I.R., Rasheed A.A., Hassan S.A.D.H., Hussein R.A., Al-Saady M. (2025). Automated aquatic biodiversity monitoring using deep learning on the Tigris River: Species identification and ecosystem assessment. International Journal of Aquatic Biology, 13(1): 30-40.

Sesta, G. (2006). Determination of sugars in royal jelly by HPLC. Apidologie, 37(1): 84-90.

Sharma M., Nandy A., Taylor N., Venkatesan S.V., Kollath V.O., Karan K., Gieg L.M. (2020). Bioelectrochemical remediation of phenanthrene in a microbial fuel cell using an anaerobic consortium enriched from a hydrocarbon-contaminated site. Journal of hazardous Materials, 389: 121845.

Thamer H.A., Saleh M.Y. (2026) Catalyst-free synthesis of polyheterocyclic compounds via UGI reactions: Structural elucidation and antileishmanial screening using promastigote viability assay. Tropical Journal of Natural Product Research, 10(2): 7150-715.

Vasumathi K.K., Premalatha M., Subramanian P. (2012). Parameters influencing the design of photobioreactor for the growth of microalgae. Renewable and Sustainable Energy Reviews, 16(7): 5443-5450.

Verawaty M., Melwita E., Apsari P., Wiyahsari M. (2017). Cultivation strategy for freshwater macro-and micro-algae as biomass stock for lipid production. Journal of Engineering and Technological Sciences, 49(2).

Vilpoux O.F., Junior J.F.S S. (2023). Global production and use of starch. In: Starchy crops morphology, extraction, properties and applications. Academic Press. pp: 43-66.

Wolkers H., Barbosa M., Kleinegris D.M., Bosma R., Wijffels R.H., Harmsen P.F.H. (2011). Microalgae: the green gold of the future. Wageningen UR.

Wong Y.C., Roma D.N. (2021). Potential of the biodegradability and characteristics of bioplastic from microalgae residues. International Journal on Algae, 23(1).

Yaseen S.N., Al-Fakhry H.H., Saleh M.Y. (2025). Local Rosuvastatin loaded by thiolated hyaluronan hydrogel for post orthodontic relapse reduction. *In Vitro* preparation and *In Vivo* assessment in rabbit. Egyptian Journal of Veterinary Sciences, 56(7): 1647-1659.

Zhang C., Li S., Ho S.H. (2021). Converting nitrogen and phosphorus wastewater into bioenergy using microalgae-bacteria consortia: a critical review. Bioresource Technology, 342: 126056.

Zhang, X., Yan, S., Tyagi, R. D., Drogui, P., & Surampalli, R. Y. (2016). Ultrasonication aided biodiesel production from one-step and two-step transesterification of sludge derived lipid. Energy, 94: 401-408.

Zhao P., Yu X., Li J., Tang X., Huang Z. (2014). Enhancing lipid productivity by co-cultivation of *Chlorella* sp. U4341 and *Monoraphidium* sp. FXY-10. Journal of Bioscience and Bioengineering, 118(1): 72-77.

Zhu S., Higa L., Barela A., Lee C., Chen Y., Du Z.Y. (2023). Microalgal consortia for waste treatment and valuable bioproducts. Energies, 16(2): 884.